NIST Technical Note 1600

Residential Structure Separation Fire Experiments

Alexander Maranghides
Erik L. Johnsson

NIST National Institute of Standards and Technology • U.S. Department of Commerce

NIST Technical Note 1600

Residential Structure Separation Fire Experiments

Alexander Maranghides
Erik L. Johnsson
U.S. Department of Commerce
Technology Administration
Building and Fire Research Laboratory
National Institute of Standards
And Technology
Gaithersburg, MD 20899

August 2008

U.S. Department of Commerce
Carlos M. Gutierrez, Secretary

National Institute of Standards and Technology
James M. Turner, Deputy Director

National Institute of Standards and Technology Technical Note 1600
Natl. Inst. Stand. Technol. Tech. Note 1600, 42 pages (August 2008)
CODEN: NSPUE2

Table of Contents

List of Figures

List of Tables

Residential Structure Separation Experiments

by

Alexander Maranghides, Erik L. Johnsson

Abstract

Building codes often allow structures with window openings and combustible exteriors to be built with as little as 1.8 m (6 ft) of separation between them. In a recent full-scale laboratory experiment at the National Institute of Standards and Technology (NIST), it took less than 80 s for flames from a simulated house with combustible exterior walls to ignite a similar "house" 1.8 m (6 ft) away. In another experiment, involving the same type of structures, the flames from one simulated house again reached the second, but this time a gypsum barrier protected the simulated home from sustained ignition. The experiments showed that an adjacent structure can be ignited if flames from a fire inside a house exit through window openings. The experiments illustrated how a fire resistant barrier can, in the scenario tested, slow down flame spread between two structures separated by 1.8 m (6 ft). The scenarios tested were not the worst case. Flame spread between structures is a complex process primarily affected by structure construction type, structure separation distance, placement and size of windows and weather conditions.

KEY WORDS: residential structures, structure separation distance, community fire spread, multi-structure fires

1.0 Background

According to the National Fire Incident Reporting System (NFIRS) [National Fire Data Center, Feb 2006], the following summarizes the statistics related to recent U.S. occurrences of fire spread between structures. In 2003, fires spreading beyond the building of origin accounted for 5.4 % of all structure fires. Between 2001 and 2003, fires that spread beyond the building of origin were responsible, on average, for 100 deaths per year, or about 11 % of all structural fire related fatalities. The costs from these fires are estimated at over $0.25 billion per year or 12 % of the total dollar loss from structure fires. See Appendix D for detailed tabulation of these statistics. Even though NFIRS does not include all fire incidents, the above data illustrates the magnitude of the problem. Fire spread between structures (when not prevented by suppression) is governed by four parameters: construction type, placement and size of windows, proximity of structures or structure separation distance, and weather conditions, specifically wind. Recent building code changes permit structures built of unrestricted construction (no enhanced fire resistance) to be separated by only 1.8 m (6 ft). As the preponderance of high density housing increases, so does the risk of fire incidents involving multiple structures.

2.0 Introduction

Fire spread between adjacent homes has always been a concern of the firefighting community, yet the effect of more dense construction and more closely built homes on fire spread has not been extensively characterized. In a recent full-scale laboratory experiment at the National Institute of Standards and Technology (NIST), it took less than 80 s for flames from a simulated house with combustible exterior walls to ignite a similar "house" 1.8 m (6 ft) away. In another experiment, involving the same type of structures, the flames from one simulated house again reached the second, but this time a gypsum barrier protected the simulated home from sustained ignition. This helps to illustrate the significance of the problem. Solving this problem would address the $0.25 billion fire losses associated with multiple structure fires.

The two experiments described above were part of a NIST Building and Fire Research Laboratory (BFRL) project to develop computer models that better predict the spread of fire in communities. The computer fire modeling and visualization programs, developed by NIST, are the Fire Dynamic Simulator (FDS) [McGrattan et al, 2007] and Smokeview [Forney, 2004]. FDS numerically models the movement of smoke and hot gases from a fire, predicting gas temperatures, heat fluxes, gas velocities and sprinkler activation times. The Smokeview program graphically depicts this information. FDS and Smokeview are beginning to be used by both fire investigators looking into why fires behave in specific ways and by builders or architects who want to know how fire detection equipment will react to fires. Data from the house-to-house fires, once incorporated into the FDS program and portrayed with the Smokeview software, will allow fire protection engineers, fire code officials and firefighters to better understand fire spread potential in dense housing communities. Fire departments are particularly interested in estimates of the time required for fire spread from one house to another. Such data would allow them to plan an appropriate and effective response.

The NIST house-to-house fire spread experiments may be of considerable interest to building code authorities and community planners due to the possible implications on public safety. In recent years, building codes often allow structures with window openings and combustible exteriors to be built with as little as 1.8 m (6 ft) separation between them. The NIST experiments duplicated the 1.8 m (6 ft) distance between structures. The experiments showed that an adjacent structure can be ignited if flames from a fire inside a house exit through window openings. The second experiment, however, demonstrated that the inclusion of a fire-resistant barrier on exterior walls can significantly delay fire spread.

The scenarios tested were not the worst case, and the experiments conducted address several but not all fire spread scenarios. Fire spread between structures is a complex process primarily affected by construction type, separation distance, placement and size of windows and effects of weather. All of these factors influence ignition and flame spread between structures.

The data collected from these experiments has been used to evaluate the NIST FDS model so it can be used to predict fire spread in residential communities with particular structures and separation distances. The findings of the two experiments will be used to determine what additional experiments and research are needed to better estimate the potential for fire spread as a function of separation distance.

3.0 Technical Approach and Experimental Design

3.1 Technical Approach

The technical approach included two indoor/laboratory experiments. The four step process is listed below:

- Design of realistic residential structure separation fixture
- Fabrication and instrumentation of laboratory experiments
- Execution of laboratory experiments
- Interpretation of experimental results

3.2 Design and Fabrication of Realistic Residential Structure Separation Fixture

For both the unrestricted and fire resistant structure experiments, the structure of fire origin, shown in Fig. 1, consisted of a 3.7 m (12 ft) by 4.3 m (14 ft) room with a 2.4 m (8 ft) high ceiling. A single 0.6 m (2 ft) by 0.9 m (3 ft) window in the center (horizontally) of the wall facing the second structure was closed and locked. This window is shown in the Fig. 1 photograph and the schematics of Figs. 2 and 3. An access door was closed, but below the door was a 0.3 m (1 ft) by 1.8 m (6 ft) vent that was continuously open. For the fire resistant structure test, two 15 cm by 20 cm floodlights were placed in the vent for visibility, decreasing the area by about 1/9. The room was furnished as described in Sec. 3.5. The schematics show the relative spacing of the furnishings.

The target wall window was offset from the structure of fire origin window to prevent flames from the fire room window from entering the target wall through its window. The target wall window was necessary for locating a heat flux gauge without breaching the structure in a way that could affect the durability of the wall.

3.3 Unrestricted Construction Experiment

Figures 4 and 5 are schematics and photographs, respectively, of the two construction techniques used in these experiments. The structure of fire origin and the target wall were both assembled using unrestricted construction, typical of many current buildings. The order of the structural layers from inside to the outside was: drywall, wood studding, oriented strand board (OSB), weather wrap, and vinyl siding. The area between wood studs was filled with fiberglass insulation.

3.4 Fire Resistant Construction Experiment

The main difference between the first and the second experiment was the introduction of a fire resistant barrier between the OSB and the weather wrap. The fire resistant barrier used on both structures was 1.3 cm (1/2 inch) drywall. Placing gypsum board on an exterior wall is not a typical construction practice for many reasons. It is, however, a simple means to demonstrate the value of a fire resistance level at least equal to what a gypsum board would provide.

Figure 1. Photograph of the side of the structure of origin facing the adjacent target wall.

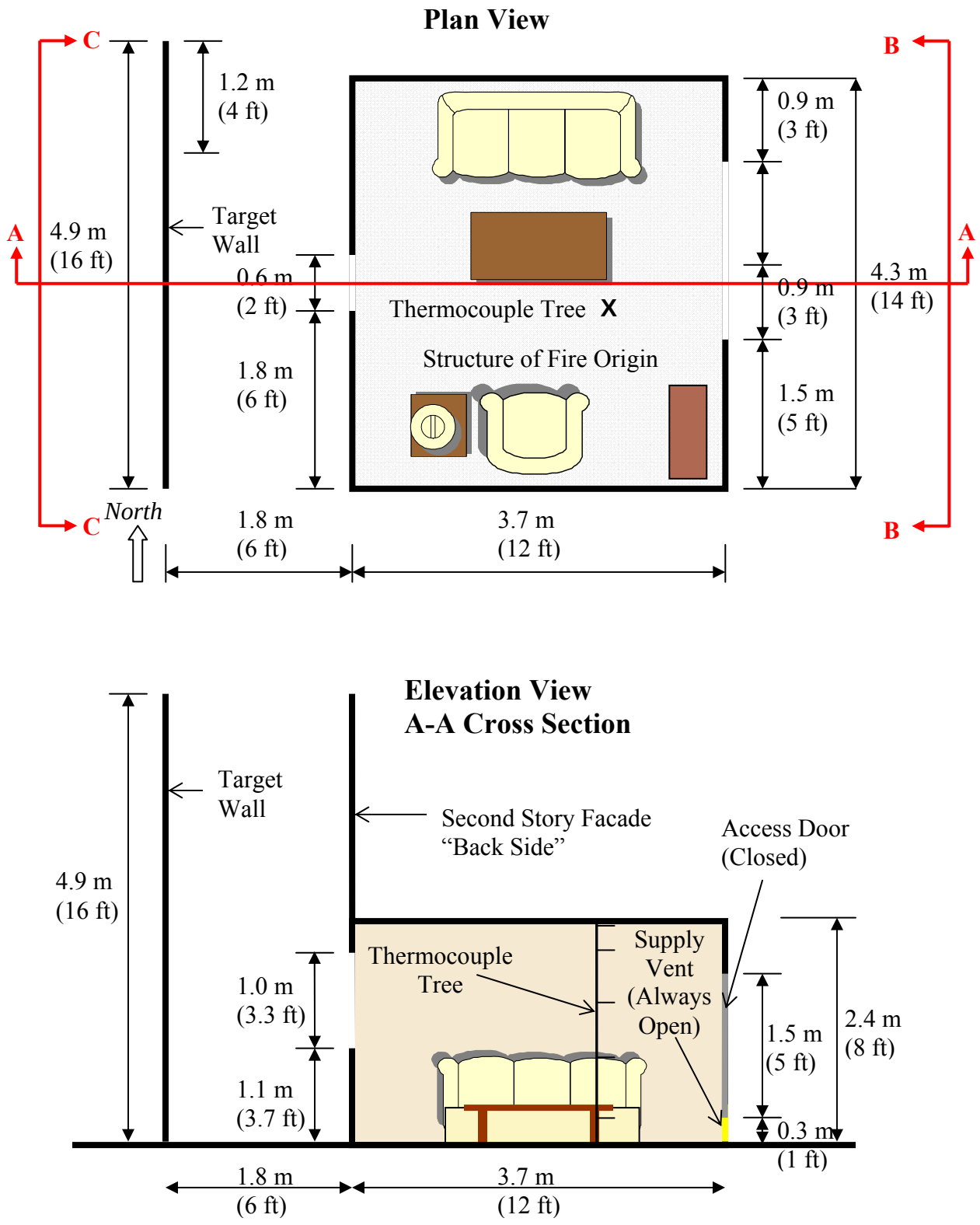

Figure 2. Plan and cross section views of the two structures (not to scale).

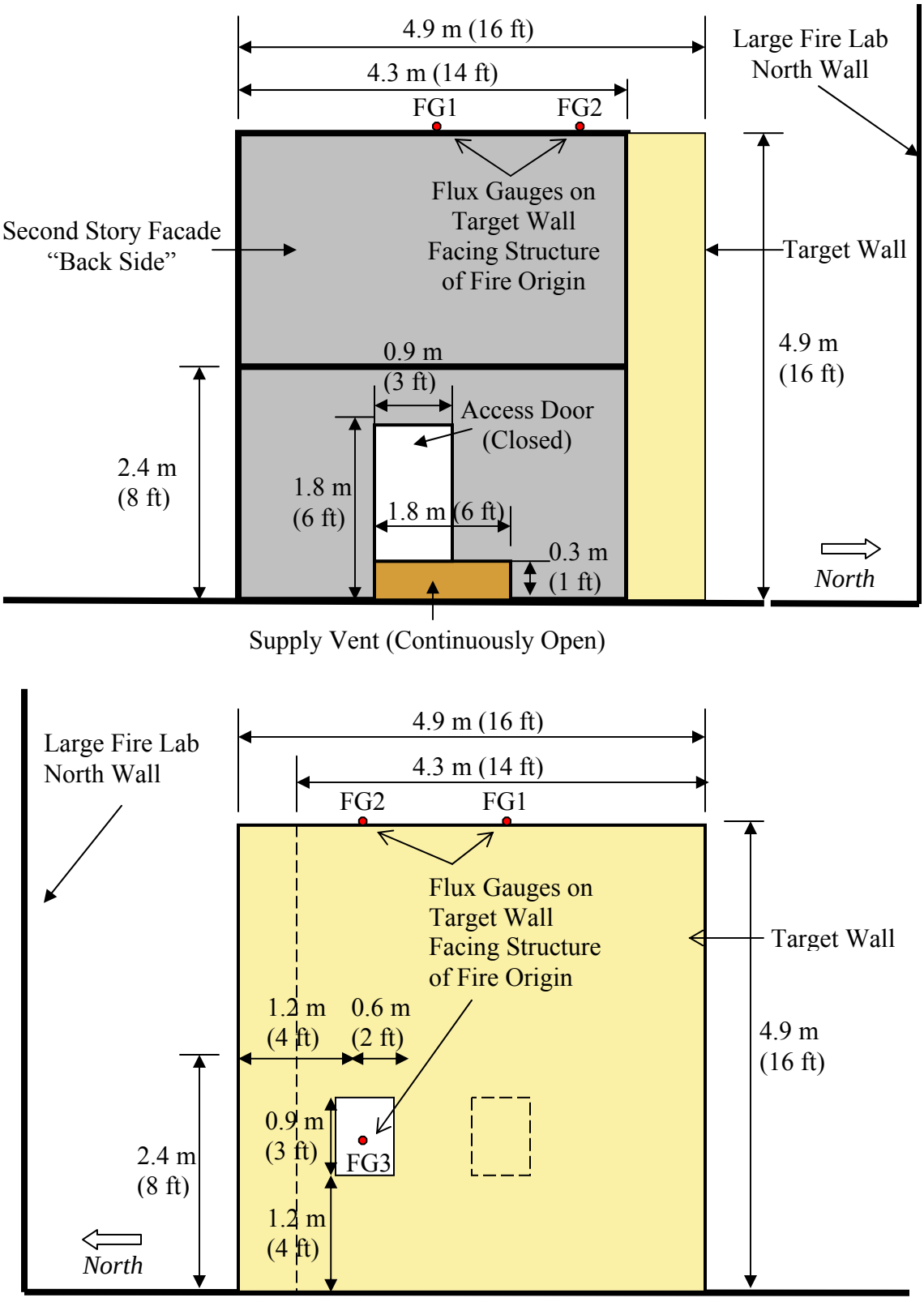

Figure 3. Cross section B-B (above) and C-C (below) of the two structures (not to scale).

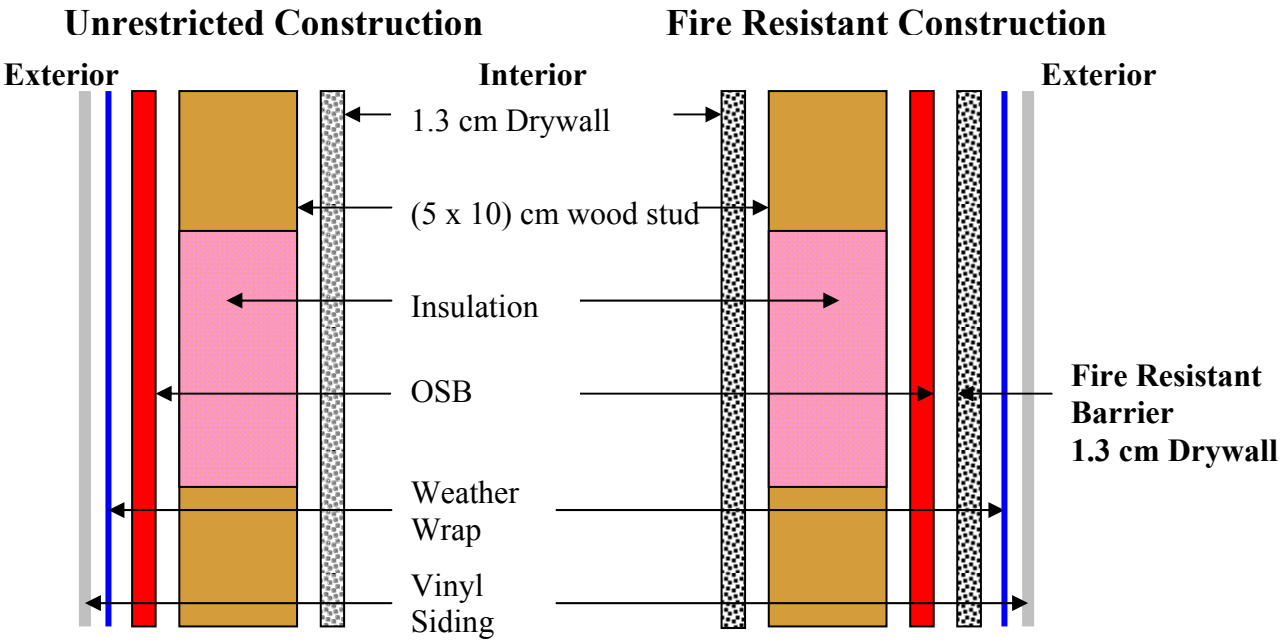

Figure 4. Schematic showing structural differences between unrestricted and fire resistant construction.

Figure 5. Photograph showing structural differences between unrestricted (left) and fire resistant (right) construction.

3.5 Structure of Fire Origin Contents

The structure of fire origin was furnished with the identical furnishings for both experiments. The "living room" type of arrangement contained a sofa, an arm char, a coffee table, an end table with a lamp and a bookcase. The interior walls were covered with wood paneling and the floor was carpeted. Table 1 contains the particulars of room contents. Figure 7 is a photograph of the interior of the structure of fire origin which shows a wall, window, curtain, some furniture, and a thermocouple tree. Figure 2 shows the locations of the major furnishings.

Table 1 Contents' descriptions and weights

Item	**Dimensions Width, Height, Length (m, m, m) (±1 %)[1]**	**Quantity**	**Combustible Material**	**Total Mass (kg) (±2 %)[1]**
Sofa	0.91, 0.74, 2.16	1	Plastics/ wood	50.6
Arm chair	0.91, 0.74, 1.00	1	Plastics	30.0
Coffee table	0.66, 0.40, 1.28	1	Wood	17.2
End Table	0.59, 0.48, 0.63	1	Wood	9.5
Bookcase	0.92, 1.82, 0.31	1	Particle board	39.7
Wall Trim	0.011, 0.087, 25.6	-	Plastic	10.0
Window Trim	0.0055, 0.0235, 3.2	-	Plastic	0.1
Wood paneling[2]	0.004, 1.22, 2.44	13	Wood	115.7
Curtain	1.0, 2.0, 0.002	1	Plastic	0.4
Carpet	3.62, 0.02, 4.24	1	Plastic	39.3
Total				**312.5**
Fuel Loading	**(19.7 ± 0.5) kg/m^2 [(4.0 ± 0.1) lbs/ft^2]^1**			

[1] Uncertainties are combined and expanded (k=2)
[2] 0.004 m thick (5/32 inch) medium density fiberboard (MDF)
Flame Spread 200 or less ASTME-84

Figure 6. Photograph showing interior of room of origin including wall, window, curtain, some furniture, and a thermocouple tree.

4.0 Experimental Measurements and Procedures

The primary objective of the experiments was to assess the impact of construction differences on the ignition of one structure by a burning adjacent structure. Two structure separation experiments (SSE) were conducted in the NIST Large Fire Laboratory (LFL). The uncertainties for the measurements described here are detailed in Appendix A. Throughout this report, uncertainties are combined with coverage factor k=2 unless otherwise stated.

4.1 9 m x 12 m Hood Description

The LFL High Bay test area is nominally 9 m (30 ft) wide and 37 m (120 ft) long. The SSE experiments were conducted under the 9 m by 12 m (30 ft by 39 ft) hood which is permanently installed in the facility. Top and side view diagrams of the hood and duct system are shown in Fig. 7. The test area beneath the hood is open on three sides, and the fourth side is near the north wall of the laboratory. The base of the hood is located 6.4 m (21 ft) above the laboratory floor. The constructed room was centered between the north and south sides of the hood.

4.2 Heat Release Rate Calorimeter

The heat release rate (HRR) was measured using oxygen consumption calorimetry in the 9 m by 12 m (30 ft by 39 ft) exhaust hood in the NIST Large Fire Laboratory. The products of

combustion from the fire filled the upper layer of the room and then flowed out of the window where they were completely captured by the exhaust hood. Measurements of the duct mass flow rate and the concentrations of various gas species were used to infer the HRR of the fire. This form of fire calorimetry was first suggested by Huggett [1980], who exploited the finding that the amount of heat released from most organic materials per unit mass of oxygen consumed in their complete combustion is nearly constant. Thus, the oxygen decrease in the duct flow (relative to ambient air) is a measure of the HRR in the flow. Huggett showed that for most common materials containing C, H, O, N, the heat release per unit mass of oxygen consumed is constant to within ±5 %. This sets a fundamental accuracy limit in this method for materials that are not chemically characterized. For fuels that are well-characterized, this parameter can be

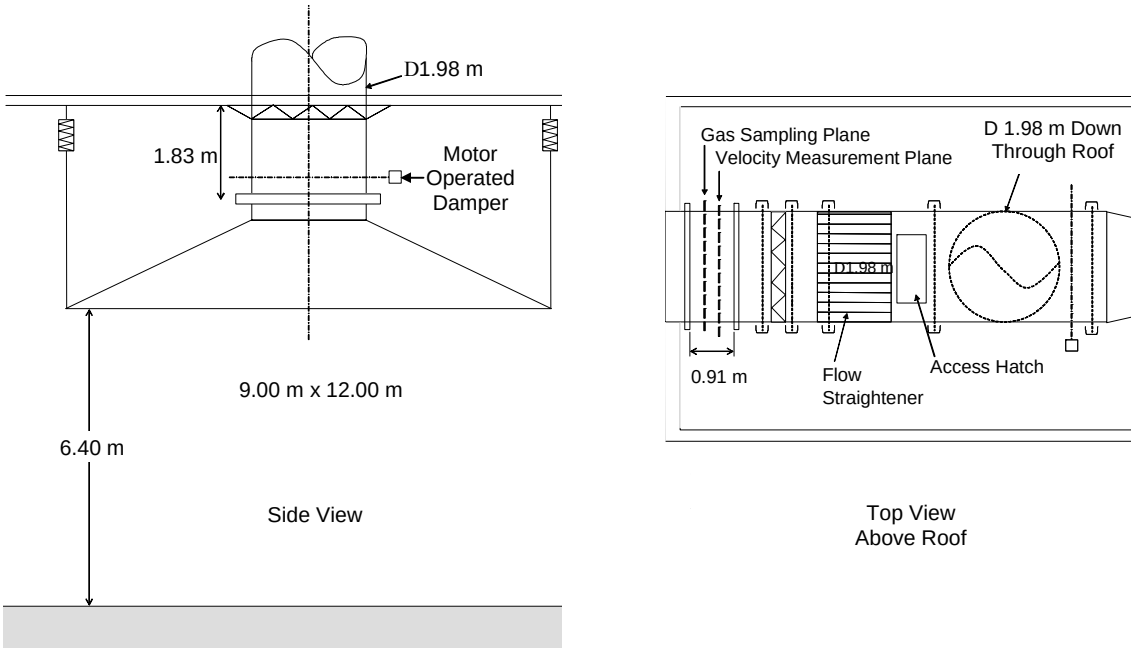

estimated with greater accuracy.

Figure 7. Large Fire Laboratory 9 m x 12 m exhaust hood and duct system

Bryant et al. [2003] describe the heat release measurement facility, instrumentation, calibration, measurement uncertainty and experimental procedures in detail. The calorimetry determination required about 40 measurements. These included temperature and pressure in the exhaust duct to quantify the total mass flow of exhaust gases and gas species sampled in the exhaust duct, transported to the instruments in a control room, and analyzed for oxygen, carbon dioxide, and carbon monoxide. Water vapor in the exhaust stream was trapped and not measured. The ambient temperature, pressure, and relative humidity in the test bay were measured and used in the HRR calculation. The computation of HRR was made following Bryant et al. [2003; 2004]. Appendix A.2 details the inputs resulting in 16.4 % HRR uncertainty for these experiments.

4.3 Temperature

The thermocouple tree for measuring temperatures in the fire room (shown in Fig. 6.) was located approximately 1.8 m (6 ft) from the south wall and 1.2 m (4 ft) from the east wall. The tree consisted of six 24 gauge type K bare-bead thermocouples. The beads were located on individual horizontal "branches" approximately 6 cm from the vertical centerline of the tree. The locations of the thermocouples relative to the ceiling were: 2.5 cm (1 in), 30.5 cm (1 ft), 61.0 cm (2 ft), 91.4 cm (3 ft), 152.4 cm (5 ft) and 213.4 cm (7 ft). The tree was suspended from the ceiling and attached to the floor with a screw to provide tension for maintaining vertical alignment. Appendix A.3 describes asymmetrical uncertainties for temperature measurements in these experiments which depend on fire condition and thermocouple location.

4.4 Heat Flux

Heat fluxes were measured only during Experiment 2. The objective of these measurements was to provide information on the incident heat flux experienced by the adjacent structure from the burning structure. Three Schmidt-Boelter total heat flux gauges were used to measure the heat fluxes generated on the target wall: two at the top of the wall and one at the target wall window. The target wall window gauge is shown in the Fig. 8 photograph. Table 2 summarizes the location, orientation, and designation of the total heat flux gauges used in these experiments.

Table 2 Location and orientation of heat flux gauges

Heat Flux Gauge	Height above Ground (m) (±1 %)	Distance from South End of Target Wall (m) (±1 %)	Location	Orientation (Horizontal Axes)
Gauge 1 SN#120295	4.9	2.3	Top of target wall	Pointing East
Gauge 2 SN#120294	4.9	3.5	Top of target wall	Pointing East
Gauge 3 SN#120297	1.4	3.5	Target wall window	Pointing East

A Schmidt-Boelter flux gauge uses a water-cooled thermopile as a sensor whose surface temperature is uniform and close to that of the cooling water used. The gauge was used to measure the combined convective and radiative heat fluxes to the sensor surface. The gauges (Medtherm Model GTW-15SB-6-60-40-484K) had a field of view of 180°. They were rated at 150 kW/m^2, and had a time response of approximately 0.1 s to 0.2 s. Signal and thermocouple wires from the gauges and cooling water supply and return lines were thermally protected using a thermal ceramic blanket and then wrapped with aluminum foil. Uncertainties were ±3 %.

4.5 Data Acquisition

The NIST Large Fire Laboratory Data Acquisition system (DAQ) was utilized to monitor HRR, heat fluxes and temperatures at a sampling rate of 1 Hz. The following description of the data acquisition system is modified from a more detailed description in Bryant et al [2004].

The signals from the various measurement devices used for oxygen-depletion calorimetry determination of heat release rate were collected using the NIST Large Fire Laboratory data acquisition system (DAQ) programmed with LabView. The DAQ was configured to collect data

both from instruments for calorimetry calculations and from other instruments or sensors being utilized for the experiment. All channels were scanned at a rate of 200 Hz and the signals were multiplexed to a single channel on the primary DAQ board. Each channel was electronically averaged for 1 s and the digital value was stored to the computer. Some signal conditioning features included an electronic filter (200 Hz low pass), gains of 100 for temperature and heat flux millivolt signals, and cold-junction compensation for thermocouples.

Figure 8: Photograph of flux gauge (FG3) in target wall window looking at structure of fire origin.

4.6 Experimental Procedure

The two experiments were conducted using similar experimental procedures. Once the structures were constructed and furnished, the instrumentation was installed. The compartment was evacuated and the compartment door was set partially open at a 30° angle. A remotely ignited book of matches was used to set fire to a newspaper on a sofa cushion. Ignition was noted and once the window broke (it was always closed), the door was closed. The first experiment was terminated when the target structure was ignited and the HRR exceeded 15 MW, the safety threshold for sustained fires in the LFL. The second experiment was allowed to burn to completion.

5.0 Experimental Results

Results and timelines for the two experiments are listed below. For this discussion, combined expanded uncertainties related to time are ±2 s.

5.1 Experiment 1 - Unrestricted Construction

At ignition, the window was closed and the access door was set partially open. The fire was initiated on one side of the sofa, and 3 min and 40 s after ignition, the window broke. The door was then secured in the closed position while the supply vent remained open providing air to the fire. The flames exiting the window impinged on the target structure within seconds. On the structure of origin, the oriented strand board located above the window was ignited shortly after the flames exited the window. On the target wall and second story facade, the vinyl siding and weather wrap melted away with minimal contribution to the total energy release since no flames were visible from them. The oriented strand board of the target wall was ignited 5 min after ignition, or 80 s after the fire exited the structure of origin. The experiment was terminated at the point that the peak heat release rate nominally reached (15.0 ± 2.5) MW. Table 3 summarizes the event times for each experiment.

Table 3 Times of events during each experiment.

Event	Unrestricted Construction Experiment 1		Fire Resistant Construction Experiment 2	
	Time (2σ uncertainty ±2 s)			
	(min:s)	(s)	(min:s)	(s)
Ignition	00:00	0	00:00	0
Window breakage	03:42	222	03:38	218
Flames begin target wall impingement	03:51	231	03:53	233
Smoke exiting structure (no flames)	Not Applicable		04:09 to 05:42	249 to 342
Flames resume	Not Applicable		05:43	343
Fire extinguished	04:57	297	14:45	885
Flame impingement duration on target wall	01:09	69	09:18	558
OSB ignited on target wall	05:00	300	OSB did not ignite	

Figure 9 shows the HRR versus time for Experiment 1. The peak HRR of (14.1 ± 2.3) MW occurred at 297 s. The structure of origin flashed over at approximately (2.5 ± 0.4) MW. The fire was extinguished 5 min after ignition; therefore the period of time that the fire HRR exceeded 2.5 MW was limited to about 99 s. The measured peak heat release rate includes contributions from the building contents and the oriented strand boards burning on the outside of both structures. Figure 10 shows a section of burned OSB from the wall of the target structure.

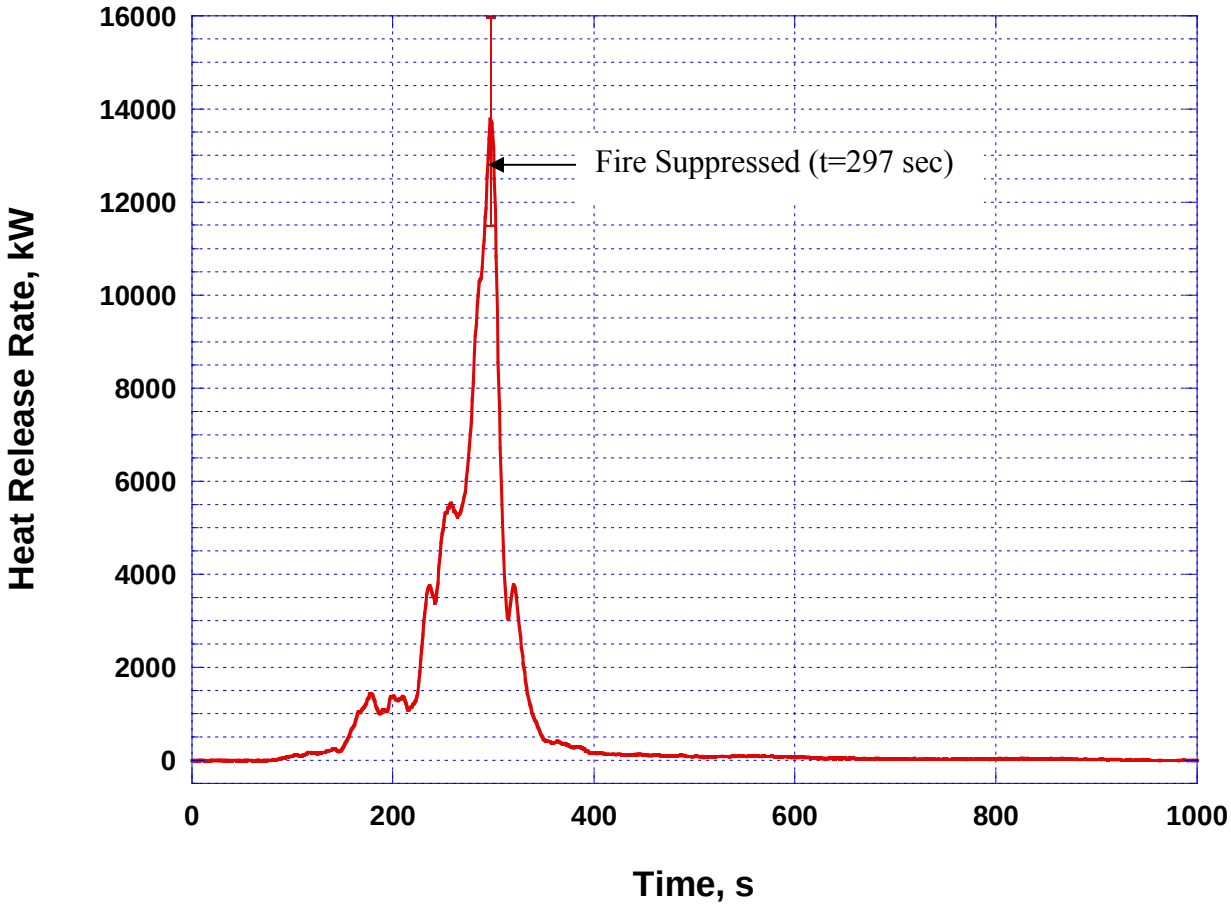

Figure 9. Experiment 1 (unrestricted construction) heat release rate versus time. Expanded uncertainty is 16.4 %.

Figure 10: Sample of burned OSB from Target Wall - Experiment 1

5.2 Experiment 2 - Fire Resistant Construction

The window failed approximately 3 min and 40 s after ignition, which was the same time as during the previous experiment. Within 15 s the flames were impinging on the target wall. The fire went through a transition period of 1 min 45 s where only hot gases (no flames) were exiting the structure. At approximately 6 min after ignition, flames resumed. At 14 min and 25 s, the fire was extinguished. In this experiment, the fire resistant barrier prevented ignition of the OSB even after approximately 9 min of direct flame impingement on the target structure. Figure 11 shows a section of unburned OSB from the wall of the target structure.

Figure 12 shows the HRR versus time for Experiment 2. The peak HRR of (10.0 ± 1.6) MW occurred at 398 s. The period of the fire that the HRR exceeded 2.5 MW totaled about 536 s.

Figure 13 shows the temperatures versus time from the thermocouple tree in the room and in the window. The temperature in the window increased to 560 °C +10/-0 °C before it broke at 3:38. The indicated window temperature dropped when the thermocouple fell with the glass, but peaked again at 613 °C +50/-0 °C when the room flashed-over. After that time, all of the thermocouples in the room measured similar temperatures with the ones near the ceiling decreasing somewhat over time.

Figure 14 shows the heat fluxes versus time. Gauges 1 and 2 were at the same height, 4.9 m (16 ft). Gauge 3 was located at the height of the window. Gauge 2 saw the flames escaping from the window and therefore experienced the largest heat flux which peaked at nearly 140 kW/m^2 and was over 50 kW/m^2 for much of the fire. Gauge 1 measured fluxes mostly in the range from 20 kW/m^2 to 70 kW/m^2. Gauge 3 measured fluxes less than 30 kW/m^2.

Figure 11: Sample of unburned OSB from Target Wall - Experiment 2

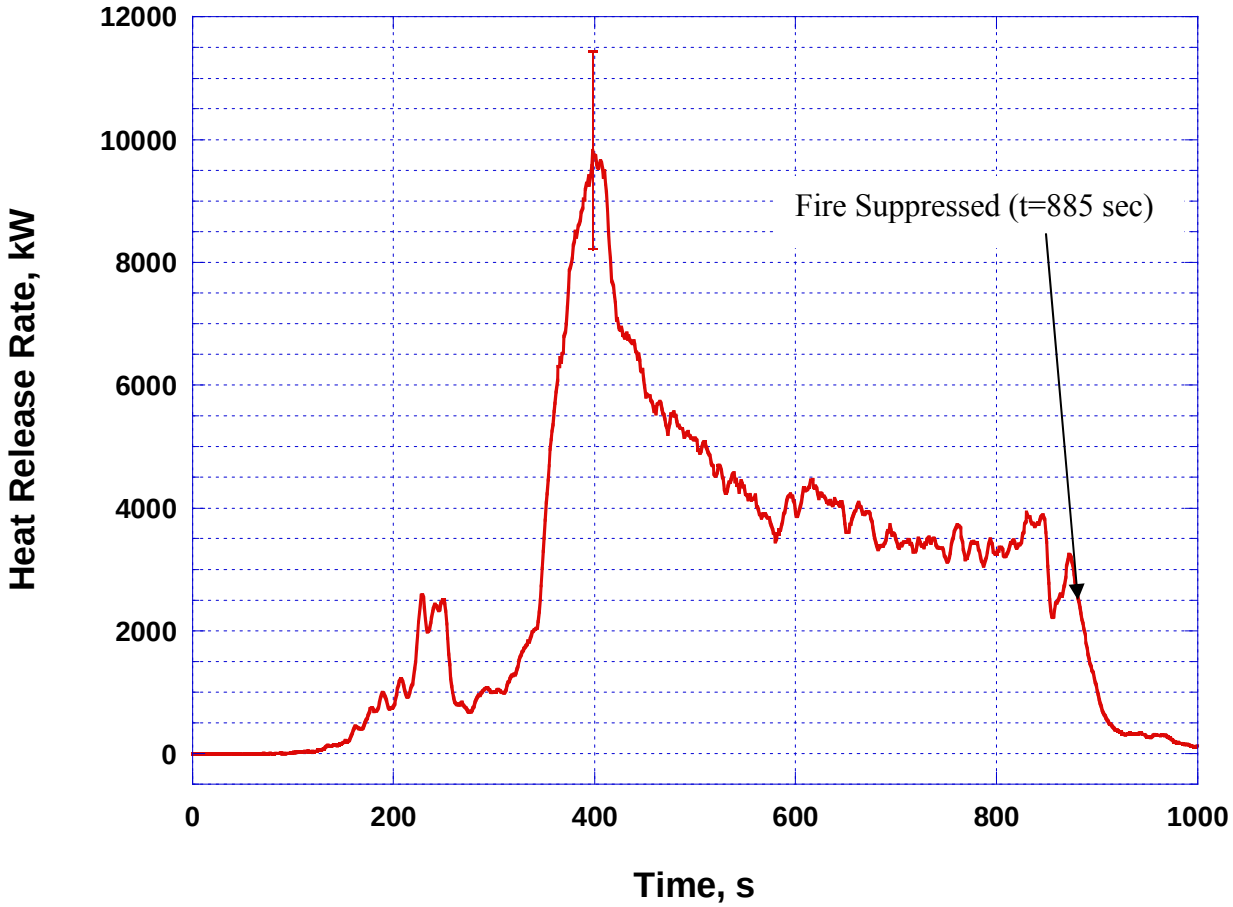

Figure 12. Experiment 2 (fire resistant construction) heat release rate versus time. Expanded uncertainty is 16.4 %.

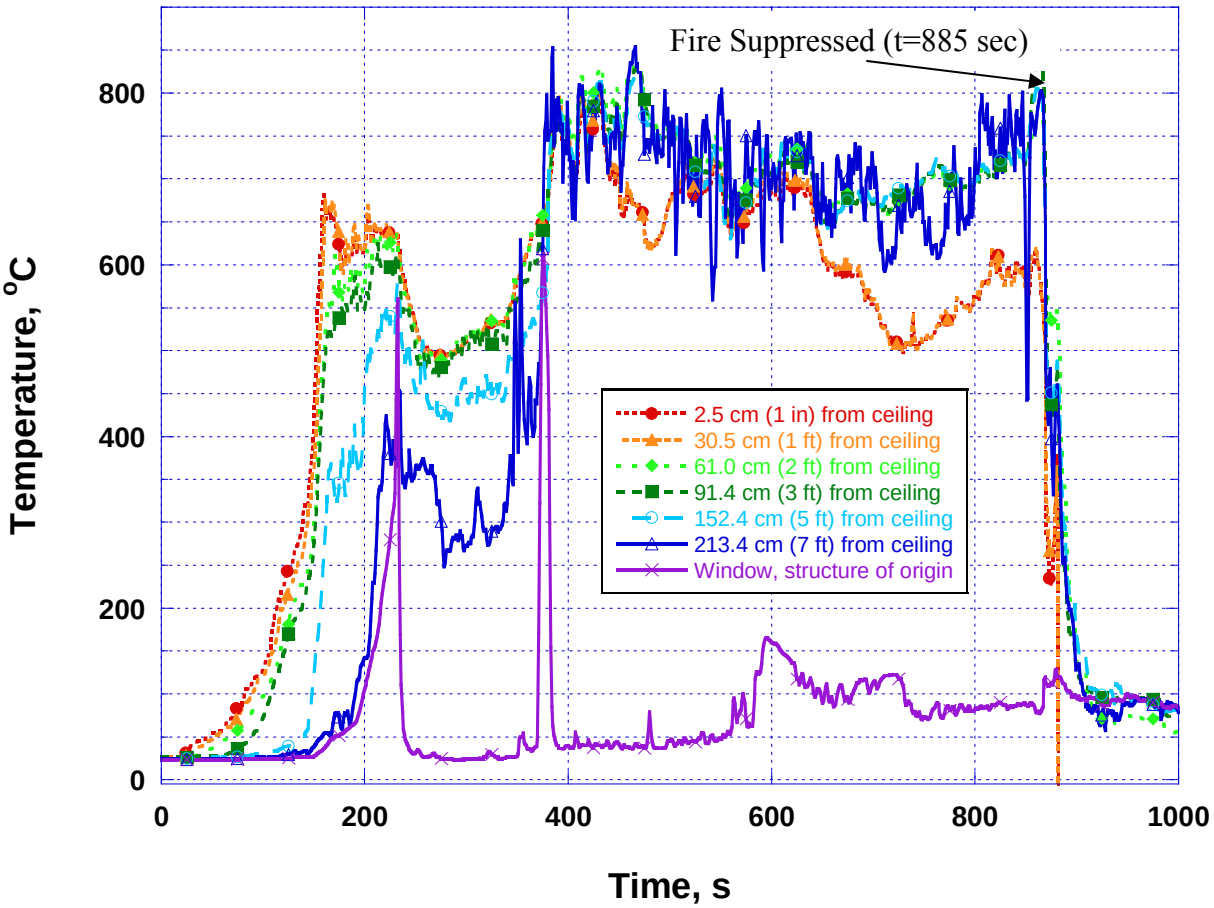

Figure 13. Experiment 2 (fire resistant construction) temperatures versus time. Data have been smoothed (5 s window). Expanded uncertainty before 380 s is about +0/-200 °C for the two thermocouples at the lowest height and +100/-0 °C for the others. After 380 s, the uncertainty for all temperatures is about +50/-0 °C.

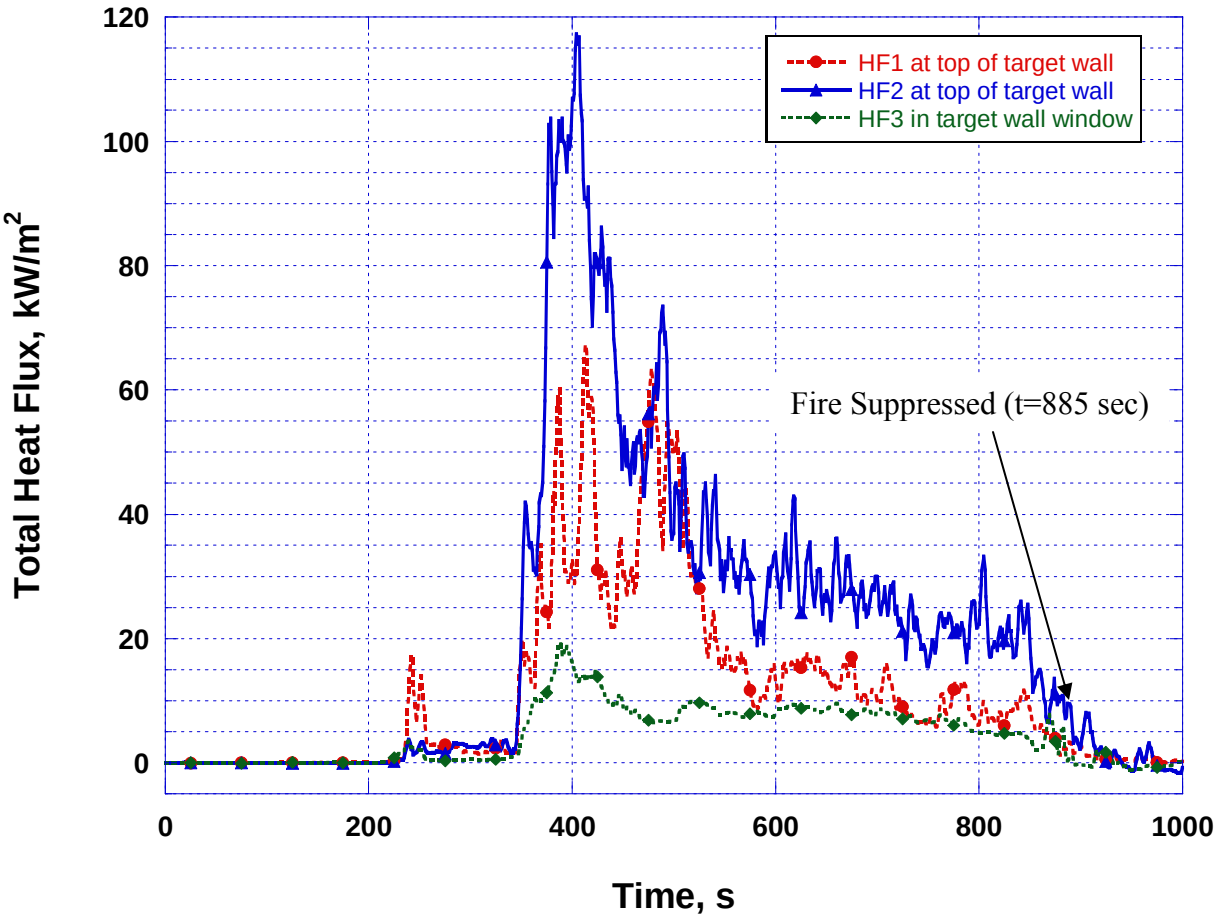

Figure 14. Experiment 2 (fire resistant construction) heat fluxes versus time. Data have been smoothed (5 s window). Relative expanded uncertainty is ±3 %.

Figure 15. Unrestricted Construction Experiment: Target Wall OSB Ignited 1 min 20 s after Window Failure

Figure 16. Fire Resistant Construction Experiment: 9 min after Window Failure – Target Wall OSB Not Ignited

6.0 Discussion of Results

It is revealing to relate the results of these experiments with the time required for the fire service to respond to a structure fire incident. In NFIRS, [National Fire Data Center, Aug 2006] response times are measured from alarm time to arrival on scene, but there is uncertainty in the data. NFIRS 5.0 defines alarm time as "when the alarm was received by the fire department." This definition is vague and subjective. Some departments may read this definition to mean when the notification comes into the 911 communications center (911 activation), while others may interpret it as when the notification comes into the station (dispatch time).Thus, depending on the interpretation by the department, response times reported to NFIRS may or may not include call processing and dispatch time, which could typically take between 30 s and 120 s.

In 2001 and 2002, as shown in Fig. 17, the highest percentage (16 %) of structure fires had a fire service response time in the 4 min range. The percent of structure fires with response times of 3 min and 5 min were not far behind at 15 % and 14 %, respectively. Overall, 61 % of structure fires in 2001 and 2002 had a response time of less than 6 min.

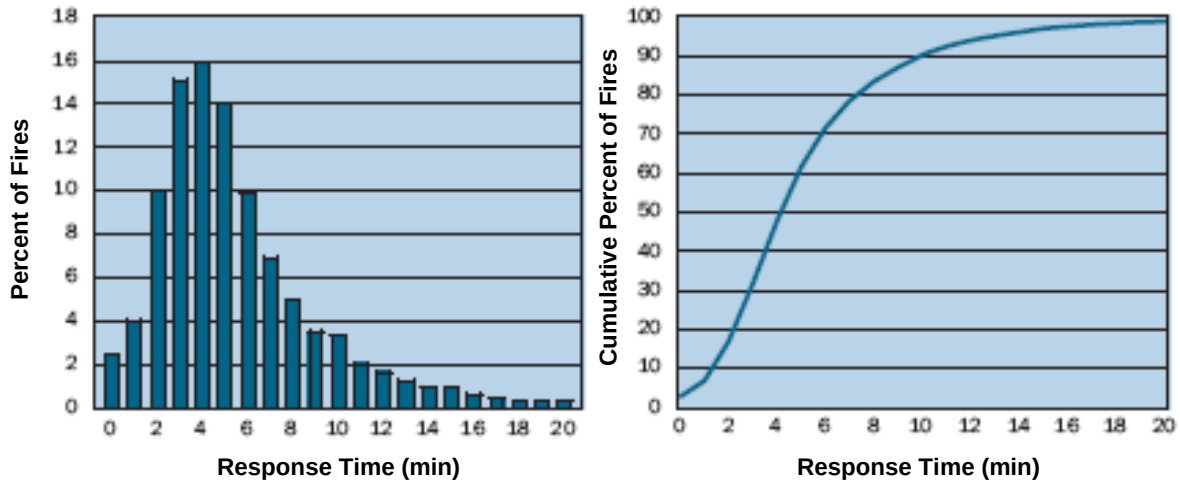

Figure 17. Fire Service Response Times to Structural Fires

The two NIST experiments provide limited information and do not represent a worst case scenario. The limited data from the two experiments illustrate the benefits of fire resistant construction in providing significant time for fire department response based on the NFIRS provided data.

6.1 Unrestricted Construction

The unrestricted construction experiment resulted in window failure at 3 min and 42 s after ignition and involvement of the adjacent structure another 1 min and 18 s later. If the fire department was notified as soon as the fire exited the structure of origin, for the unrestricted construction scenario, less than 10 % of the fire departments would be able to arrive on the scene in 80 s, before the second structure was on fire. Alternatively, in the most extreme case, if the

fire department was notified immediately upon ignition, approximately 55 % of fire departments would be able to get on the scene in 5 min, before fire spread to an adjacent structure.

6.2 Fire Resistant Construction

The fire resistant construction experiment resulted in window failure at 3 min and 42 s after ignition. The fire did not spread to the adjacent structure even after 9 min of flame impingement. During that experiment the fuel load of the structure of origin only provided enough energy for 9 min of flame impingement on the adjacent structure. In a real world scenario, it is likely that the exposure duration would have been longer. The additional protection provided by the fire resistant construction would provide critical time for fire department response. If adjacent structure ignition was assumed after 9 min of flame exposure, a conservative assumption, and if the fire department was notified after window failure, over 85 % of fire departments would be on the scene by that time.

7.0 Summary

The primary objective of the NIST Community Fire Spread Project is to develop tools that assess and predict the risk of communities and structures to Wildland-Urban Interface (WUI) fires. These tools will be based on computer models of fire spread and smoke transport as well as data sets derived from experiments conducted in NIST's Large Fire Laboratory and in the field.

Two experiments were conducted at NIST to investigate fire spread between adjacent structures. In both experiments, the structures were separated by 1.8 m (6 ft). The first experiment with unrestricted construction resulted in ignition of the adjacent structure in 5 min after ignition, or 80 s after the structure of fire origin was breached. The second experiment was conducted with fire resistant construction that prevented ignition of the adjacent structure. There are a number of options with respect to fire resistant material selection, and no attempt has been made to provide any materials recommendations at this time. The two experiments have demonstrated that fire resistant construction can significantly reduce the overall flame spread risk in communities where structures are placed in close proximity to each other. Even though NFIRS does not contain information on all fire incidents, the available fire department response data suggests that the delayed flame spread between adjacent structures associated with fire resistant construction can provide significant valuable time for fire department response.

The NIST Community Scale Fire Spread project [Rehm et al] will continue investigating fire propagation in communities. Additional model input and validation experiments are being planned to further develop the community scale prediction capabilities of the NIST FDS fire model.

8.0 Acknowledgements

The authors would like to acknowledge Matt Bundy of NIST for conducting the calorimeter calibration, Bradley S. Pabody of the United States Fire Administration for the NFIRS data. Laurean DeLauter, Ed Hnetkovsky, Jack Lee and Gale Miller of NIST were instrumental in the construction of the experimental enclosures and Robert Anleitner of Geo-Centers Inc. provided data acquisition support. Dr. Dave Evans of the Society of Fire Protection Engineers (and formerly of NIST) deserves credit for initiating these experiments.

9.0 References

Bryant, R., Ohlemiller, T., Johnsson, E., Hamins, A., Grove, B., Guthrie, W.F., Maringhides, A.and Mulholland, G., The NIST 3 Megawatt Quantitative Heat Release Rate Facility, *NIST Special Publication 1007*, National Institute of Standards and Technology. Gaithersburg, MD, December 2003.

Bryant, R., Ohlemiller, T., Johnsson, E., Hamins, A., Grove, B., Guthrie, W.F., Maringhides, A.and Mulholland, G., The NIST 3 Megawatt Quantitative Heat Release Rate Facility – Description and Procedures, *NISTIR 7052*, National Institute of Standards and Technology, Gaithersburg, MD, September 2004.

Bundy, M., personal communication, National Institute of Standards and Technology, Gaithersburg, MD, April 2008.

Forney, G.P. and McGrattan, K.B. User's Guide for Smokeview Version 4: A Tool for Visualizing Fire Dynamics Simulation Data, *NIST Special Publication 1017,* National Institute of Standards and Technology, Gaithersburg, MD, 2004, http://fire.nist.gov/bfrlpubs/

Hamins, A.; Maranghides, A.; McGrattan, K. B.; Johnsson, E. L.; Ohlemiller, T. J.; Donnelly, M. K.; Yang, J. C.; Mulholland, G. W.; Prasad, K. R.; Kukuck, S. R.; Anleitner, R. L.; McAllister, T. P., Experiments and Modeling of Multiple Workstations Burning in a Compartment. Federal Building and Fire Safety Investigation of the World Trade Center Disaster, *NIST NCSTAR 1-5B*; National Institute of Standards and Technology, Gaithersburg, MD, 352 p, Sept 2005.

Huggett, C., "Estimation of the Rate of Heat Release by Means of Oxygen Consumption," *Journal of Fire and Materials*, 12: 61-65 (1980).

Janssens M.;Parker, W. J., "Oxygen Consumption Calorimetry," *Heat Release in Fires*, Babrauskas, V., Grayson, S. J., Eds. (E & FN Spon.), pp. 31-59 London, UK, 1995.

McGrattan, K. B.;Hostikka, S.;Floyd, J. E.; Baum, H. R.; Rehm, R. G. Fire Dynamics Simulator (Version 5), "Technical Reference Guide", *NIST Special Publication 1018-5*, National Institute of Standards and Technology, Gaithersburg, MD, Oct 2007.

McGrattan, K. B.; Klein, B.; Hostikka, S.; Floyd, J. E. Fire Dynamics Simulator (Version 5), "Users Guide", *NIST Special Publication 1019-5*, National Institute of Standards and Technology, Gaithersburg, MD, Oct 2007, http://fire.nist.gov/bfrlpubs/

Mulholland, G. "The emission and optical properties of smoke", *Recent Advances in Flame Retardancy of Polymeric Materials*, Vol. 3, pp. 22-29 (1992)

National Fire Data Center, *National Fire Incident Reporting System (NFIRS) Database*, U.S. Fire Administration, Feb 2006, http://www.usfa.dhs.gov/fireservice/nfirs/index.shtm.

National Fire Data Center, *Structure Fire Response Times Topical Fire Research Series,* Volume 5 – Issue 7, U.S. Fire Administration, January 2006 / Revised August 2006.

Parker, W. J., "Calculations of the Heat Release Rate by Oxygen Consumption for Various Applications," *Internal report NBSIR 81-2427*, National Bureau of Standards (NBS), Gaithersburg, MD, 1982.

Rehm, R. G.; Hamins, A.; Baum, H. R.; McGrattan, K. B.; Evans, D. D., Community-Scale Fire Spread, *NIST IR 6891,* National Institute of Standards and Technology, Gaithersburg, MD; July 2002.

Taylor, B. N.; C. E. Kuyatt, Guidelines For Evaluating and Expressing the Uncertainty of NIST Measurement Results. *NIST-TN 1297*, National Institute of Standards and Technology, Gaithersburg, MD; September 1994.

Walton, W.D., McElroy, J., Twilley, W.H., Hiltabrand, R.R. (1994) Smoke Measurements Using a Helicopter Transported Sampling Package, *Proceedings of the 17th Artic and Marine Oil Spill Program (AMOP) Technical Seminar,* Vol. 1, June 8-10, 1994, Vancouver, British Columbia.

APPENDIX A. – Uncertainty Analysis

A.1 General

There are different components of uncertainty in the data for each of the measurement types reported here. Uncertainties are grouped into two categories according to the method used to estimate them. Type A uncertainties are evaluated by statistical methods, and Type B are evaluated by other means [Taylor and Kuyatt, 1994]. Type B analysis of systematic uncertainties involves estimating the upper (+ a) and lower (- a) limits for the quantity in question such that the probability that the value would be in the interval (± a) is essentially 100 %. After estimating uncertainties by either Type A or B analysis, the uncertainties are combined in quadrature to yield the combined standard uncertainty. Multiplying the combined standard uncertainty by a coverage factor of two results in the total expanded uncertainty that corresponds to a 95 % confidence interval (2σ). Portions of the uncertainty analyses are taken from Bryant [2003, 2004].

A.2 Heat Release Rate

Bryant et al. [2003; 2004] discuss the analytical equations, the calibration procedures, and the methods used to determine the HRR and its uncertainty for calorimetry in the NIST 6 m by 6 m (20 ft by 20 ft) exhaust hood. The instrumentation and uncertainty analysis is analogous to Bryant et al. [2003; 2004] for calorimetry in the 9 m by 12 m hood (29 ft by 39 ft), which was used for these experiments. The largest contribution to the measurement uncertainty is due to the determination of the mass flow in the exhaust duct [Bryant et al., 2004]. Parker [1982] and Janssens and Parker [1995] discuss the details of the HRR calculation based on the extent to which the duct gas flow is characterized.

Calibration burns using natural gas were conducted in the time frame surrounding the series of experiments to assess the accuracy of the HRR measurement and to characterize its repeatability. Burning a substance such as a gaseous fuel at a controlled rate provides an independent measurement of HRR to compare to the measurement by oxygen consumption calorimetry. A natural gas burner with active flow control was employed [Bryant et al., 2003]. Calibration experiments were performed 12 weeks before the experiments. The burner was placed directly under the 9 m by 12 m (29 ft by 39 ft) exhaust hood. During the calibration, the heat output of the burner was held constant for 2 min to 5 min at each setting. For this calibration, the expanded uncertainty of the natural gas HRR using oxygen depletion calorimetry was estimated as 15.6 %. This uncertainty resulted from combining, in quadrature, the general uncertainty of the LFL calorimetry method (11 %), the variation in the calibration factor (10.8 %), and the uncertainty in the calorific value of the natural gas (2.5 %). The calorific value variation was over a six-month period, as determined by examination of gas chromatographic concentration measurements provided by the natural gas supplier, the Washington Gas Company.

For the SSE experiments, an additional 5 % expanded uncertainty was added in quadrature to reflect the unknown oxygen depletion characteristics of the fuels burned in the structures. Huggett [1980] determined that the 5 % variation captured the burning characteristics of most fuels. The resulting expanded 2σ uncertainty for HRR measured in the SSE experiments was 16.4 %.

The calorimetric HRR measurements were corrected for baseline drift which was likely due to the instability of the oxygen analyzer. For Experiment 1, this baseline drift correction ranged from about 8 kW to 9 kW. For Experiment 2, the correction ranged from 17 kW to 84 kW. The corrections were performed by calculating a linear equation for the drift using the HRR recorded with no fire before and well after the part of the experiment experiencing combustion. These corrections did not have a significant impact on the HRR uncertainty.

It should be noted that more recent experimentation has shown some sensitivity of the 9 m x 12 m hood calorimetry to the location of the fire plume under the hood. [Bundy, 2008] This has not been characterized or quantified sufficiently to include it in these uncertainty estimates.

Finally, there is an additional uncertainty in the HRR measurement related to the time response of the system to brief events. The system time response is about 10 s so any HRR peaks or valleys that are shorter in duration than 10 s will have a measured amplitude (relative to the base or background average) somewhat less than the true amplitude.

A.3 Temperature

Type K thermocouples was used with an inherent standard uncertainty of 2 °C (4 °F) based on the manufacturer's specification. The expanded uncertainty (95 % confidence interval) with a coverage factor of two is 4 °C (8 °F). The uncertainty due to A/D conversion is an order of magnitude less than this and is thus neglected.

Additional uncertainties in measured temperature are primarily due to radiative heating and cooling of the thermocouple bead that causes it to respond to phenomena other than the surrounding gas temperature. Generally, thermocouples located in a hot upper layer will measure temperatures cooler than the actual gas temperature due to some radiative losses at the bead. Thermocouples in cooler locations that receive radiation from the fire or hot upper layer will read higher than the actual gas temperature. The error caused by the radiative environment is generally much greater for thermocouples located in cool locations than for those in hot locations.

The thermal environment surrounding a given thermocouple is very difficult to characterize. Generally, temperatures measured in the hot upper layer were estimated to be less than 100 °C lower than the real temperatures. Before the room flashed over, the temperatures in the lower layer were estimated to be less than 200 °C too high. After flashover, all temperatures were likely within 50 °C of the true gas temperatures because the environment surrounding the thermocouples became much more uniform which decreased radiative gains and losses. These uncertainties overwhelm the inherent uncertainties in the thermocouple described earlier.

A.4 Heat Flux

The main sources of uncertainty pertaining to the total heat flux are: (1) the uncertainty of the A/D conversion, (2) uncertainty in the calibration, and (3) uncertainty due to soot deposition on the sensing surface of the gauge. The uncertainty in A/D conversion is inherent to the data acquisition system. It is system specific and is associated with the digitization of the analog

signals from the gauge. This type of uncertainty was taken as negligible. The calibration from the heat flux gauge manufacturer was obtained using water at 23 ºC ± 3 ºC. The relative expanded uncertainty reported by the manufacturer is ± 3 % of the gauge sensitivity (the slope of the calibration curve) with a coverage factor of 2. This would result in an uncertainty of about 4 kW/m^2 for a nominal reading of 140 kW/m^2.

Initial background heat fluxes in the absence of fire were subtracted from the gross heat fluxes measured by the DAQ. These background levels were (0.73, 0.75, and 0.87) kW/m^2 for gauges 1, 2, and 3, respectively. These offsets could be due to using cooling water of a different temperature than at calibration. Since the offsets were constant and correctible, they don't result in additional uncertainty in the measurement.

The uncertainty due to soot deposition is more difficult to quantify. The amount of soot deposition depends on many parameters, such as the location of the gauge, the flow field and temperature fields near the gauge, the duration of an experiment, and the soot volume fraction. No attempt was made to quantify this soot effect for these experiments. Since flame impingement on the gauges was, at most, intermittent and brief, the additional uncertainty is considered negligible.

APPENDIX B. – Data (only in electronic form, available upon request)

Heat Release Rate, Heat Flux, Temperature

APPENDIX C. – Calorimeter Calibration Report

Filename(s):	(1) 042804_9mCalVer(1) (2) 042804_9mCalVer(2)
Lab:	NIST LFL
Date:	4/28/2004
Start Time:	(1) 8:42 AM; (2) 1:24 PM
Operator:	JL
Hood Size (m):	9 x 12
Hood Calibration Factor (Ave, Std Dev):	(1) 0.914, 0.059; (2) 0.887, 0.038; (combined) 0.900, 0.049
Heat Release Rate Range Used to Determine Calibration Factor (MW)	0.6 to 10
Exhaust Volume Flow Rate (m3/s):	(1) 40.6; (2) 41.4
Exhaust Mass Flow Rate (kg/s):	(1) 50.1; (2) 50.6
HRR Correction Due to Ambient Oxygen Drift:	(1) HRR_{corr}(kW)=0.01728(t-7620)+25.4 (2) HRR_{corr}(kW)=0.03594(t-3033)+8.4
Fuel Net HOC per unit Oxygen (MJ/kg O_2):	12.52

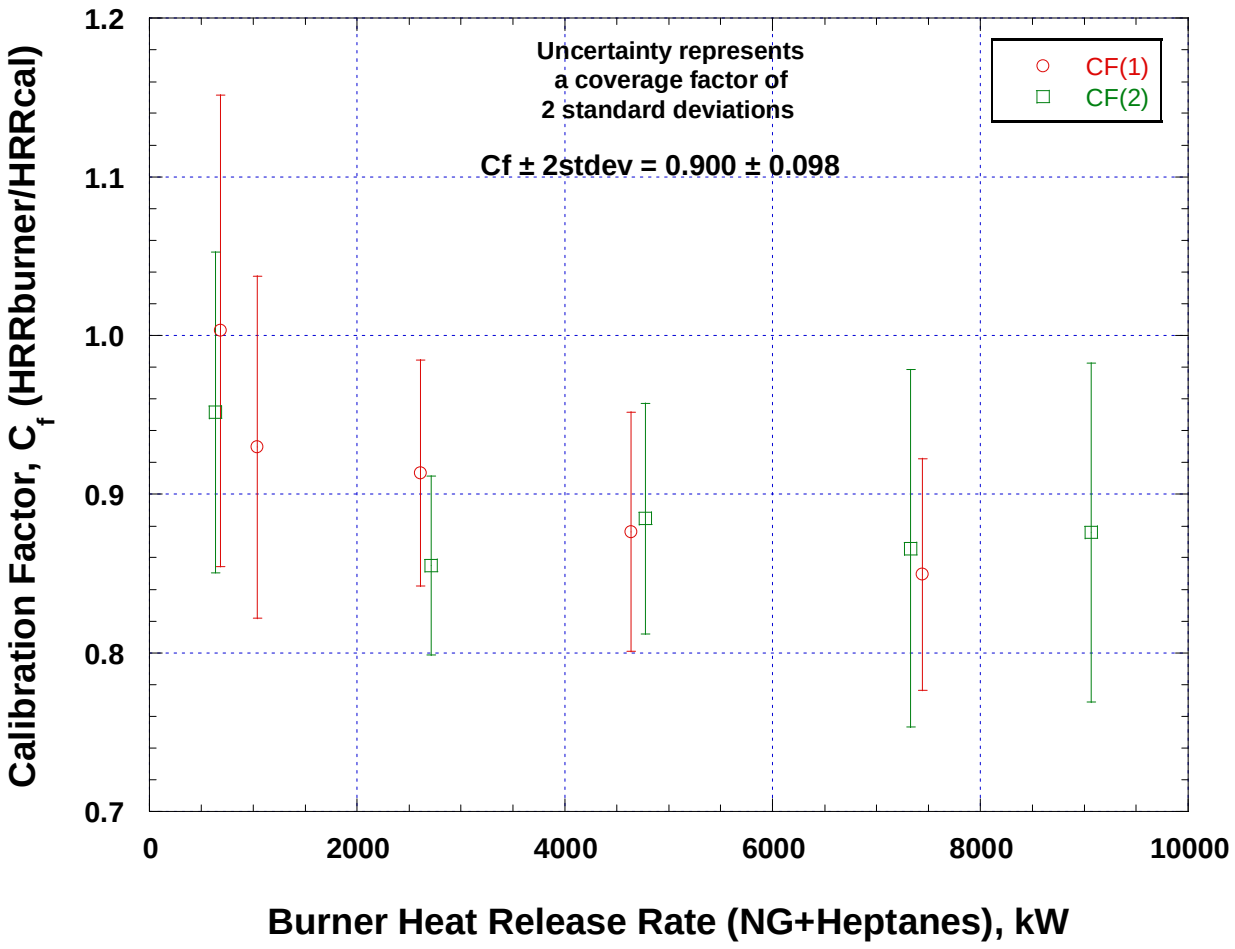

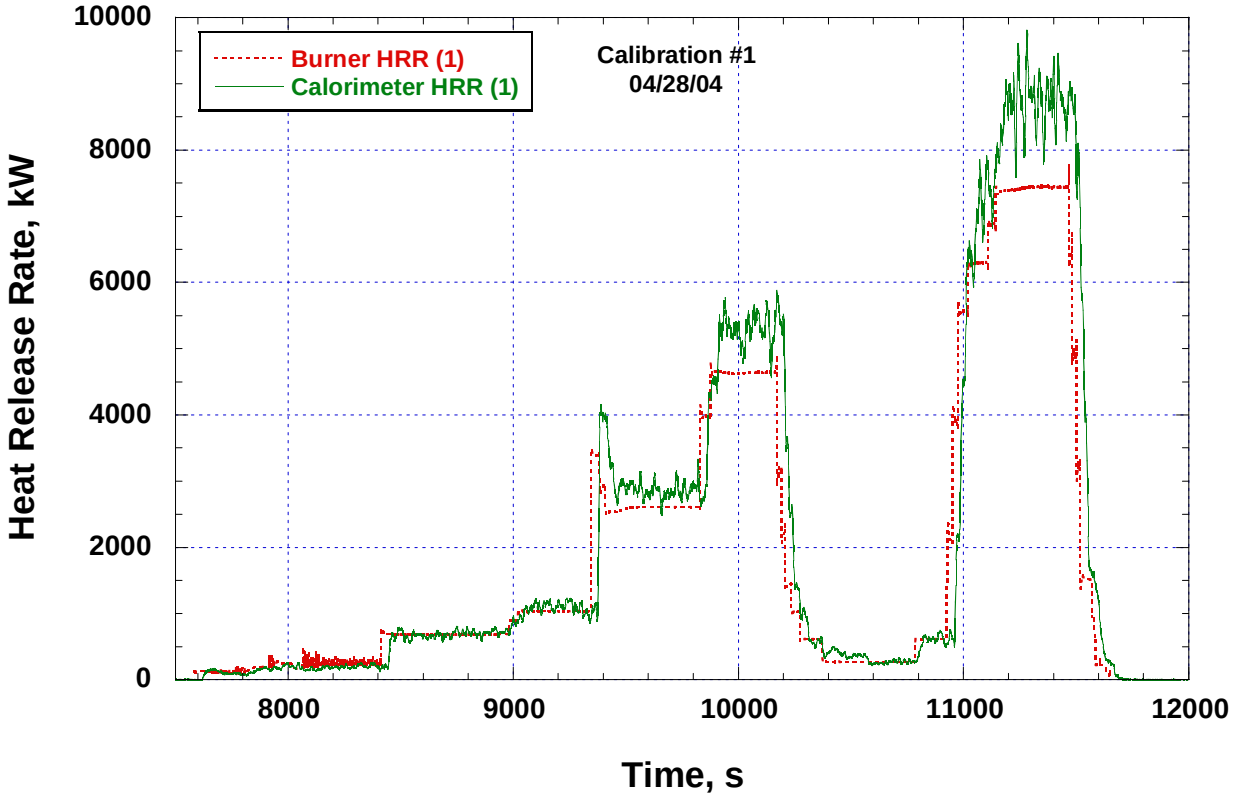
Burner HRR (1)
Calorimeter HRR (1)
Calibration #1
04/28/04
Heat Release Rate, kW
Time, s
0
2000
4000
6000
8000
10000
8000
9000
10000
11000
12000

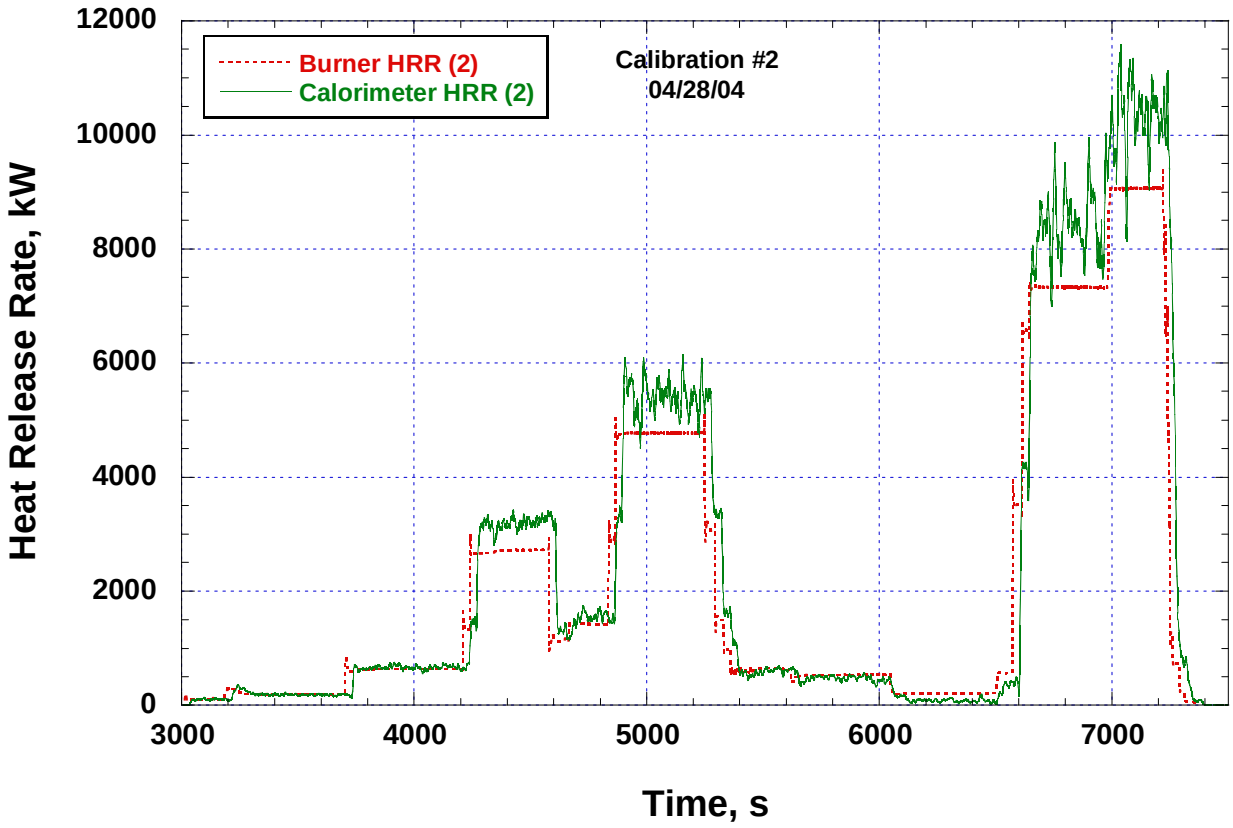
Burner HRR (2)
Calorimeter HRR (2)
Calibration #2
04/28/04
Heat Release Rate, kW
Time, s
12000
10000
8000
6000
4000
2000
0
3000
4000
5000
6000
7000

APPENDIX D. – NFIRS Data

NFIRS Fire Tally Report
BY: FIRE SPREAD

February 28, 2006
12:54 PM

2003 NFIRS Data
United States Fire Administration
National Fire Data Center

WHERE: struc_type BETWEEN '1' AND '2' AND (aid != '3' AND aid != '4')

Descriptor	FIRE_SPRD	Frequency	%	Deaths	%	Injuries	%	Dollar Loss	%
FIRE SPREAD		76	0.1%	0	0%	0	0%	$287,110	0%
Confined to object of origin	1	37,225	31.7%	71	7%	901	17.6%	$220,392,624	9%
Confined to room of origin	2	32,632	27.8%	138	13.5%	1,876	36.7%	$271,727,439	11.1%
Confined to floor of origin	3	8,254	7%	103	10.1%	557	10.9%	$216,124,079	8.8%
Confined to building of origin	4	32,710	27.9%	580	56.9%	1,453	28.5%	$1,399,343,256	57%
Beyond building of origin	5	6,351	5.4%	127	12.5%	319	6.2%	$346,691,842	14.1%
Category Totals	**FIRE_SPRD**	**117,248**	**100%**	**1,019**	**100%**	**5,106**	**100%**	**$2,454,566,350**	**100%**

NFIRS Fire Tally Report
BY: FIRE SPREAD

February 28, 2006
12:56 PM

2002 NFIRS Data
United States Fire Administration
National Fire Data Center

WHERE: struc_type BETWEEN '1' AND '2' AND (aid != '3' AND aid != '4')

Descriptor	FIRE_SPRD	Frequency	%	Deaths	%	Injuries	%	Dollar Loss	%
FIRE SPREAD		20,269	24.6%	55	7.7%	599	15.8%	$143,530,632	7.6%
Confined to object of origin	1	6,321	7.7%	10	1.4%	114	3%	$21,220,589	1.1%
Confined to room of origin	2	22,591	27.4%	100	14%	1,360	35.9%	$205,436,127	10.8%
Confined to floor of origin	3	5,546	6.7%	86	12.1%	365	9.6%	$152,439,160	8%
Confined to building of origin	4	23,187	28.1%	379	53.2%	1,143	30.2%	$1,147,688,704	60.4%
Beyond building of origin	5	4,554	5.5%	82	11.5%	207	5.5%	$228,898,294	12.1%
Category Totals	**FIRE_SPRD**	**82,476**	**100%**	**712**	**100%**	**3,788**	**100%**	**$1,899,216,106**	**100%**

NFIRS Fire Tally Report

BY: FIRE SPREAD

February 28, 2006
12:58 PM

2001 NFIRS Data

United States Fire Administration
National Fire Data Center

WHERE: struc_type BETWEEN '1' AND '2' AND (aid != '3' AND aid != '4')

Descriptor	FIRE_SPRD	Frequency	%	Deaths	%	Injuries	%	Dollar Loss	%
FIRE SPREAD		16,476	27.1%	35	6%	467	17.7%	$116,142,116	8.6%
Confined to object of origin	1	5,024	8.3%	14	2.4%	79	3%	$27,382,932	2%
Confined to room of origin	2	14,952	24.6%	76	13.1%	856	32.5%	$126,517,714	9.4%
Confined to floor of origin	3	3,751	6.2%	46	7.9%	263	10%	$110,988,097	8.2%
Confined to building of origin	4	16,929	27.9%	327	56.5%	777	29.5%	$805,798,247	59.7%
Beyond building of origin	5	3,587	5.9%	81	14%	192	7.3%	$163,667,011	12.1%
Category Totals	**FIRE_SPRD**	**60,728**	**100%**	**579**	**100%**	**2,634**	**100%**	**$1,350,514,317**	**100%**